Effective-medium theory for anisotropic magnetic metamaterials

Junfeng Jin,[1,*] Shiyang Liu,[1] Zhifang Lin,[1] and S. T. Chui[2]
[1]*Surface Physics Laboratory, Department of Physics, Fudan University, Shanghai 200433, China*
[2]*Bartol Research Institute, University of Delaware, Newark, Delaware 19716, USA*
(Received 6 May 2009; revised manuscript received 29 June 2009; published 1 September 2009)

We have developed an effective-medium theory within the coherent-potential approximation, which is especially suitable to retrieve the effective constitutive parameters (permittivity and permeability) of the anisotropic magnetic metamaterials consisting of the ferrite rods. The anisotropy originates from the gyromagnetic property of the ferrite material whose permeability is a tensor with nonzero off-diagonal components. To confirm the validity of our method the photonic band structures of the two-dimensional periodic magnetic metamaterials are calculated, which are in agreement with the effective-medium theory in the long wavelength limit, in addition, even when $a/\lambda_0 \sim 0.4$ the effective-medium theory can still be applied, where a and λ_0 are the lattice constant and the vacuum wavelength, respectively. The simulations on the electric field patterns for a plane wave illuminated on the magnetic metamaterials and the equal-size effective scattering objects are performed, the results corroborate the effectiveness of the effective-medium theory once again. We also perform the simulation for the metamaterial composed of disordered ferrite rods, which is still in agreement with the effective-medium theory, suggesting the powerfulness of the effective-medium theory. Moreover, our results suggest that the anisotropy must be considered exactly in order to retrieve the effective constitutive parameters accurately.

DOI: 10.1103/PhysRevB.80.115101 PACS number(s): 42.70.Qs, 41.20.Jb, 76.50.+g, 78.20.Ci

I. INTRODUCTION

Metamaterials are composite structured materials composed of subwavelength building blocks, which exhibit novel and unique electromagnetic (EM) properties, not occurring in nature. A particularly important class of such materials is the negative refractive-index metamaterials (NIM).[1,2] Since the first realization of the NIM by Smith *et al.*,[3] various new samples are proposed and proved to possess the negative refractive index.[4–9] To investigate and characterize the optical properties of the metamaterials, it is crucial to retrieve the effective constitutive parameters (permittivity and permeability). Many works have been done to deal with the issue and great progress has been made,[10–16] among which homogenization scheme for bianisotropic metamaterials is brought forward.[16] However, since most metamaterials designed base on the Pendry's scheme, concretely, an array of metallic wires to provide negative permittivity[17] and an array of split-ring resonators to provide negative permeability,[18] most theories developed are particularly applied to such systems.

Very recently, it has been demonstrated that a novel metamaterial consisting of only the ferrite rods exhibit excellent negative refractive behavior.[8] The optical properties of the thus designed NIM is magnetically tunable, it is, therefore, a magnetic metamaterial (MM). Since the gyromagnetic property of the ferrite material, its magnetic permeability is a tensor with nonzero off-diagonal components. Different from the anisotropy originated from the geometric asymmetry, the MM is from the material itself, consequently, it is intrinsic. Therefore, to retrieve the complete optical properties of the MM, the anisotropy must be considered from the beginning of the effective-medium theory (EMT). The gyromagnetic property of the ferrite material has important implications, it can lead to the broken of the time-reversal symmetry, which is a critical aspect to design the one-way waveguide.[19]

The present work is devoted to develop an EMT especially for the anisotropic MM in two dimensions. The gyromagnetic property is considered exactly in the theory, the effective constitutive parameters can be easily obtained by applying the analytical equations obtained from the EMT. In addition, it can be recovered to that for the metamaterials consisting of the isotropic dielectric rods after simplification.[14] To corroborate the effectiveness of our method, the band structures have been calculated within the multiple-scattering method, which are in good agreement with the EMT. The electric field patterns have been simulated as well for a real MM, an effective equal-size object, and also a real MM with position disorder introduced, which suggest that the consideration of the anisotropy is necessary to retrieve the genuine optical properties of the MM.

II. EMT FOR ANISOTROPIC MM

In this section, we present the formulation of the EMT for anisotropic MM in two-dimensional (2D) case, generalization to three dimensions is straightforward. The system is made up of the ferrite rods arranged in a periodic structure such as square lattice or hexagonal lattice. It should be pointed out that even when the position disorder is introduced, the method is still applicable. For convenience, we take square lattice as an example to expatiate the theory. The geometry of the system is illustrated in Fig. 1 where the base vectors $|\boldsymbol{a_1}|=|\boldsymbol{a_2}|=a$ with a the lattice constant. The ferrite rods with permittivity ε_s and tensor permeability $\hat{\mu}$ are arranged periodically in the isotropic homogeneous medium (supposed to be air for convenience) with permittivity ε_0 and permeability μ_0. The rod axes are along z direction and the radii of the ferrite rods are r_s. The gyromagnetic permeability of the ferrite rods bears the form[20]

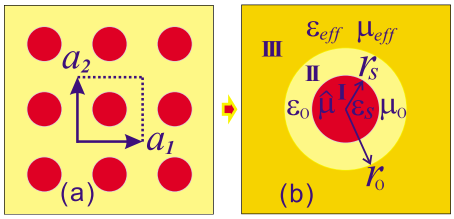

FIG. 1. (Color online) (a) A 2D anisotropic MM consisting of the ferrite rods arranged periodically in the air background and (b) its corresponding geometry in the effective-medium theory. The red circles, light yellow region, and dark yellow region correspond to the ferrite rods, the isotropic homogeneous background, and effective medium, respectively.

$$\hat{\mu} = \begin{pmatrix} \mu_r & -i\mu_\kappa & 0 \\ i\mu_\kappa & \mu_r & 0 \\ 0 & 0 & 1 \end{pmatrix}, \quad \hat{\mu}^{-1} = \begin{pmatrix} \mu_r' & -i\mu_\kappa' & 0 \\ i\mu_\kappa' & \mu_r' & 0 \\ 0 & 0 & 1 \end{pmatrix} \tag{1}$$

with

$$\mu_r = 1 + \frac{\omega_m(\omega_0 - i\alpha\omega)}{(\omega_0 - i\alpha\omega)^2 - \omega^2}, \quad \mu_r' = \frac{\mu_r}{\mu_r^2 - \mu_\kappa^2},$$

$$\mu_\kappa = \frac{-\omega_m\omega}{(\omega_0 - i\alpha\omega)^2 - \omega^2}, \quad \mu_\kappa' = \frac{-\mu_\kappa}{\mu_r^2 - \mu_\kappa^2}, \tag{2}$$

where $\omega_0 = 2\pi\gamma H_0$ is the ferromagnetic resonance frequency with γ the gyromagnetic ratio, H_0 is the sum of the external magnetic field and shape anisotropy field; $\omega_m = 2\pi\gamma M_s$ is the characteristic frequency with M_s the saturation magnetization; α is the damping coefficient; and ω is the circular frequency of the incident EM wave.

The scenarios of the EMT are as follows: (i) transform the discrete periodic system in Fig. 1(a) into the effective medium with effective constitutive parameters $\varepsilon_{\mathrm{eff}}$ and μ_{eff} in Fig. 1(b); (ii) take the unit cell of the MM as an equal-area coated rod with ferrite rod as the inner core and the background medium as the coated layer with radius $r_0 = a/\sqrt{\pi}$ for the ferrite rods arranged as a square lattice, similarly, for the MM with ferrite rods arranged as hexagonal lattice, the corresponding radius of the coated layer is $r_0 = (\sqrt[4]{3}/\sqrt{2\pi})a$; (iii) the effective constitutive parameters $\varepsilon_{\mathrm{eff}}$ and μ_{eff} are determined by the condition that the total scattering of a coated rod in the effective medium vanishes in the long wave limit $k_{\mathrm{eff}} r_0 \ll 1$ where $k_{\mathrm{eff}} = k_0\sqrt{\varepsilon_{\mathrm{eff}}}\sqrt{\mu_{\mathrm{eff}}}$ with k_0 the wave number in the vacuum.[8,21,22] Actually, the EMT is still applicable even when $k_{\mathrm{eff}} r_0$ is not very small, which can be confirmed from our results thereafter. The concept of our theory is the so-called coherent-potential approximation,[22] which has been used to retrieve the effective isotropic parameters for the EM,[14,23] acoustic,[24] and even elastic metamaterials.[25]

In the 2D EM system, both the transverse electric (TE) mode and the transverse magnetic (TM) modes are the eigenmodes. For the TE mode the polarization of the magnetic field is along z direction, parallel to the external magnetic field, implying an isotropic constant permeability as can be seen from Eq. (1). Different from the TE mode, for the TM mode the magnetic field polarizes in the xy plane, perpendicular to the external magnetic field, resulting in the precessing of the magnetic dipoles in the ferrite. Consequently, anisotropy is involved for the TM mode, this is the case to be considered in present work. For the TE mode, the effective constitutive parameters have been given in the literature within the similar scheme.[14]

The theory is carried out in a similar manner as that of the Mie theory. First, expand the EM waves in regions I, II, and III of Fig. 1(b) by vector cylindrical wave functions (VCWFs)

$$\boldsymbol{L}_n^{(J)}(k,\boldsymbol{r}) = \left[\frac{dz_n^{(J)}(\rho)}{d\rho}\boldsymbol{e}_r + \frac{in}{\rho}z_n^{(J)}(\rho)\boldsymbol{e}_\phi\right]e^{in\phi}, \tag{3a}$$

$$\boldsymbol{M}_n^{(J)}(k,\boldsymbol{r}) = \left[\frac{in}{\rho}z_n^{(J)}(\rho)\boldsymbol{e}_r - \frac{dz_n^{(J)}(\rho)}{d\rho}\boldsymbol{e}_\phi\right]e^{in\phi}, \tag{3b}$$

$$\boldsymbol{N}_n^{(J)}(k,\boldsymbol{r}) = z_n^{(J)}(\rho)e^{in\phi}\boldsymbol{e}_z \tag{3c}$$

with k as the wave vector, $\boldsymbol{r} = r\cos\phi\boldsymbol{e}_x + r\sin\phi\boldsymbol{e}_y$ as the position vector, $\rho = kr$, $z_n^{(J)}(\rho)$ as the Bessel function, $J_n(\rho)$ and the first kind of Hankel function $H_n^{(1)}(\rho)$ for $J=1$ and 3, respectively. For the EM field in the region I, namely, in the ferrite rod

$$\boldsymbol{E}_s(k_s,\boldsymbol{r}) = \sum_n q_n^s \boldsymbol{N}_n^{s(1)}, \tag{4a}$$

$$\boldsymbol{H}_s(k_s,\boldsymbol{r}) = \sum_n \frac{k_s}{i\omega} q_n^s [i\mu_{\kappa s}'\boldsymbol{L}_n^{s(1)} + \mu_{rs}'\boldsymbol{M}_n^{s(1)}], \tag{4b}$$

where $k_s = k_0\sqrt{\varepsilon_s}\sqrt{\mu_s}$ with $\mu_s = (\mu_{rs}^2 - \mu_{\kappa s}^2)/\mu_{rs} = 1/\mu_{rs}'$, μ_{rs} and $\mu_{\kappa s}$ are given in Eq. (2), and the superscript s means k_s is involved in VCWFs. In the coated layer area, i.e., in region II the corresponding EM field components are

$$\boldsymbol{E}_b(k_0,\boldsymbol{r}) = \sum_n [q_n^0\boldsymbol{N}_n^{0(1)} - b_n^0\boldsymbol{N}_n^{0(3)}], \tag{5a}$$

$$\boldsymbol{H}_b(k_0,\boldsymbol{r}) = \sum_n \frac{k_0}{i\omega\mu_0}[q_n^0\boldsymbol{M}_n^{0(1)} - b_n^0\boldsymbol{M}_n^{0(3)}], \tag{5b}$$

where the superscript 0 implies k_0 is involved in VCWFs. Finally, in region III, we have

$$\boldsymbol{E}_e(k_{\mathrm{eff}},\boldsymbol{r}) = \sum_n [q_n^e\boldsymbol{N}_n^{e(1)} - b_n^e\boldsymbol{N}_n^{e(3)}], \tag{6a}$$

$$\boldsymbol{H}_e(k_{\mathrm{eff}},\boldsymbol{r}) = \sum_n \frac{k_{\mathrm{eff}}}{i\omega}\{q_n^e[i\mu_{\kappa e}'\boldsymbol{L}_n^{e(1)} + \mu_{re}'\boldsymbol{M}_n^{e(1)}] - b_n^e[i\mu_{\kappa e}'\boldsymbol{L}_n^{e(3)} + \mu_{re}'\boldsymbol{M}_n^{e(3)}]\}, \tag{6b}$$

where the superscript e implies k_{eff} is involved in VCWFs, μ_{re}' and $\mu_{\kappa e}'$ are defined by μ_{re} and $\mu_{\kappa e}$ according to Eq. (2) with μ_{re} and $\mu_{\kappa e}$ the effective tensor permeability components to be evaluated.

By matching the standard boundary conditions at $r = r_0$, it can be obtained that

$$\begin{pmatrix} q_n^e \\ b_n^e \end{pmatrix} = \mathcal{F}\begin{pmatrix} \mathcal{A}_{11} & \mathcal{A}_{12} \\ \mathcal{A}_{21} & \mathcal{A}_{22} \end{pmatrix}\begin{pmatrix} q_n^0 \\ b_n^0 \end{pmatrix} \tag{7}$$

with prefactor $\mathcal{F}=\pi/(2i\mu_0\mu_{re}')$ and the matrix elements

$$\mathcal{A}_{11} = -k_0r_0J_n'(k_0r_0)H_n^{(1)}(k_{\text{eff}}r_0) + n\mu_0\mu_{\kappa e}'J_n(k_0r_0)H_n^{(1)}(k_{\text{eff}}r_0) + k_{\text{eff}}r_0\mu_0\mu_{re}'J_n(k_0r_0)H_n^{(1)\prime}(k_{\text{eff}}r_0), \tag{8a}$$

$$\mathcal{A}_{12} = k_0r_0H_n^{(1)\prime}(k_0r_0)H_n^{(1)}(k_{\text{eff}}r_0) - n\mu_0\mu_{\kappa e}'H_n^{(1)}(k_0r_0) \times H_n^{(1)}(k_{\text{eff}}r_0) - k_{\text{eff}}r_0\mu_0\mu_{re}'H_n^{(1)}(k_0r_0)H_n^{(1)\prime}(k_{\text{eff}}r_0), \tag{8b}$$

$$\mathcal{A}_{21} = -k_0r_0J_n'(k_0r_0)J_n(k_{\text{eff}}r_0) + n\mu_0\mu_{\kappa e}'J_n(k_0r_0)J_n(k_{\text{eff}}r_0) + k_{\text{eff}}r_0\mu_0\mu_{re}'J_n(k_0r_0)J_n'(k_{\text{eff}}r_0), \tag{8c}$$

$$\mathcal{A}_{22} = k_0r_0H_n^{(1)\prime}(k_0r_0)J_n(k_{\text{eff}}r_0) - n\mu_0\mu_{\kappa e}'H_n^{(1)}(k_0r_0)J_n(k_{\text{eff}}r_0) - k_{\text{eff}}r_0\mu_0\mu_{re}'H_n^{(1)}(k_0r_0)J_n'(k_{\text{eff}}r_0), \tag{8d}$$

where $k_0=\omega/c$ corresponds to the vacuum wave number, and $k_{\text{eff}}=k_0\sqrt{\varepsilon_{\text{eff}}}\sqrt{\mu_{\text{eff}}}$ with ε_{eff} the effective permittivity and μ_{eff} the effective isotropic permeability defined as[20,26]

$$\mu_{\text{eff}} = \frac{\mu_{re}^2 - \mu_{\kappa e}^2}{\mu_{re}} \tag{9}$$

according to the matrix elements μ_{re} and $\mu_{\kappa e}$ of the effective-tensor permeability with the form of Eq. (1).

According to rule (iii) of the EMT, the coated rod located in the effective medium in Fig. 1(b) subjects to null scattering, in other words, the total-scattering cross section of the coated rod should be zero. According to the Mie theory, it is given by[14,27]

$$C_{\text{sca}} = \frac{4}{k_{\text{eff}}}\sum_n |D_n^e|^2, \tag{10}$$

where $D_n^e=b_n^e/q_n^e$ are the Mie scattering coefficients of the coated rod in the effective medium. In the limit $k_{\text{eff}}r_0 \ll 1$, C_{sca} is dominated by $n=0,\pm1$ terms in Eq. (10). Accordingly, only the angular momentums 0 and ±1 need to be considered in the EMT. Different from the isotropic case, for the ferrite rod the Mie coefficients D_{-1}^e and D_1^e are not the same. Taking account of $D_n^e=b_n^e=0$, it is straightforward to get

$$\frac{\mathcal{A}_{21}}{\mathcal{A}_{22}} = -\frac{b_n^0}{q_n^0} = -D_n^s, \quad n=0,\pm1 \tag{11}$$

from Eq. (7), where D_n^s are the Mie coefficients of the inner-core ferrite rod, which are given by

$$D_n^s = \frac{k_0r_sJ_n(k_sr_s)J_n'(k_0r_s) - \mu_0J_n(k_0r_s)j}{k_0r_sH_n^{(1)\prime}(k_0r_s)J_n(k_sr_s) - \mu_0H_n^{(1)}(k_0r_s)j} \tag{12}$$

with

$$j = n\mu_{\kappa s}'J_n(k_sr_s) + k_sr_s\mu_{rs}'J_n'(k_sr_s),$$

where r_s is the radius of the inner-core ferrite rod, and μ_{rs}' and $\mu_{\kappa s}'$ are given in Eq. (2).

Equation (11) is the master equation of the EMT for anisotropic MM. It can be simplified in the long wavelength limit. Suppose $k_{\text{eff}}r_0 \ll 1$ and $k_0r_0 \ll 1$, we can make approximations on $J_n(x)$, $J_n'(x)$, $H_n^{(1)}(x)$, and $H_n^{(1)\prime}(x)$ in $\mathcal{A}_{21}$ and $\mathcal{A}_{22}$ with $x=k_{\text{eff}}r_0$ or k_0r_0 for convenience. Then we have

$$J_0(x) \simeq 1, \quad J_1(x) \simeq \frac{x}{2},$$

$$J_0'(x) \simeq -\frac{x}{2}, \quad J_1'(x) \simeq \frac{1}{2},$$

$$H_0^{(1)}(x) \simeq 1 + \frac{2i}{\pi}\ln x, \quad H_1^{(1)}(x) \simeq \frac{x}{2} - \frac{2i}{\pi x},$$

$$H_0^{(1)\prime}(x) \simeq -\frac{x}{2} + \frac{2i}{\pi x}, \quad H_1^{(1)\prime}(x) \simeq \frac{1}{2} + \frac{2i}{\pi x^2}.$$

Taking consideration of $z_{-n}^{(J)}=(-1)^n z_n^{(J)}$, we can make approximations for the corresponding terms with negative angular momentum, where $J=1,3$ correspond to J_n and $H_n^{(1)}$, respectively. With all these approximations, we can obtain the simplified equations determining the effective permittivity ε_{eff} and the effective permeability μ_{eff},[8]

$$\varepsilon_{\text{eff}} = (1-f)\varepsilon_0 + f\tilde{\varepsilon}_s, \tag{13a}$$

$$\frac{\mu_{\text{eff}} - \mu_0}{\mu_{\text{eff}} + \mu_0} = f\frac{\tilde{\mu}_s - \mu_0 - \xi}{\tilde{\mu}_s + \mu_0 + \xi}, \tag{13b}$$

where f is the filling fraction with $f=r_s^2/r_0^2$ and

$$\tilde{\varepsilon}_s = 2\varepsilon_sF_2(x_s), \quad F_2(x_s) = J_1(x_s)/[x_sJ_0(x_s)],$$

$$\tilde{\mu}_s = \mu_sG_2(x_s), \quad G_2(x_s) = J_1(x_s)/[x_sJ_1'(x_s)],$$

$$\xi = -\frac{(1-f)\mu_0^2(\mu_\kappa/\mu_r)^2(\tilde{\mu}_s/\mu_s)^2}{(1-f)\mu_0 + (1+f)\tilde{\mu}_s}$$

with $x_s=k_sr_s$. It is noted that if μ_κ is set to be zero, Eq. (13) can be recovered to that for the isotropic case.[14]

III. EFFECTIVE CONSTITUTIVE PARAMETERS AND PHOTONIC BANDS

With the EMT developed we have calculated the effective constitutive parameters for an anisotropic MM composed of the periodically (square lattice with lattice constant $a=8$ mm) arranged ferrite rods with the radii $r_s=\frac{1}{4}a=2$ mm, the permittivity $\varepsilon_s=15$, and the saturation magnetization $M_s=1750$ Oe. The effective permittivity ε_{eff} and permeability μ_{eff} are calculated with the anisotropic MM under the magnetic field $H_0=500$ Oe. The results are shown in Fig. 2(b) where the red solid line and the blue dashed line correspond to ε_{eff} and μ_{eff}, respectively. To confirm the validity of the results the corresponding photonic band structure is calculated with the multiple-scattering method (MST) as shown in Fig. 2(a). It should be pointed out that for the simulta-

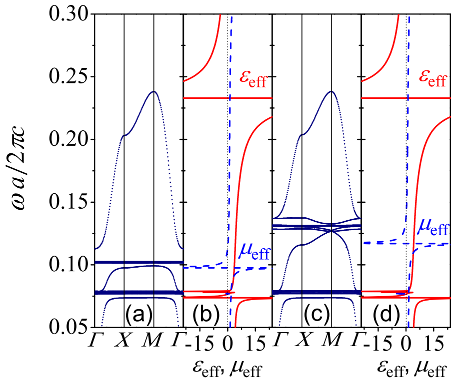

FIG. 2. (Color online) In the low-frequency range $\omega a/2\pi c \in [0.05, 0.3]$ the photonic band structures calculated with the MST are presented for the anisotropic (a) and isotropic (c) MM, respectively, the corresponding effective constitutive parameters calculated with the EMT are presented as well in (b) and (d) for the anisotropic and isotropic MM, respectively, where the red solid lines represent the effective permittivity and the blue dashed lines represent the effective permeability.

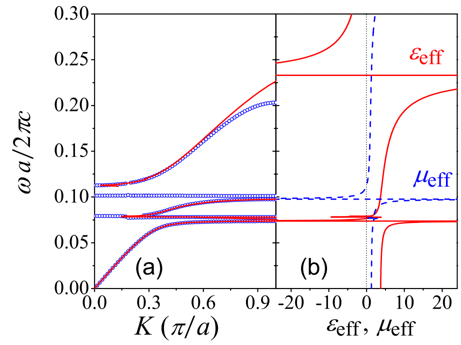

FIG. 3. (Color online) The photonic band structures calculated with the MST and the EMT, denoted with blue circles and red solid lines, respectively (a). The effective constitutive parameters calculated with the EMT are presented as well (b) for the comparison with (a) where the red solid line and the blue dashed line denote the effective permittivity and permeability, respectively.

neous positive or negative constitutive parameters,[8] there appear photonic bands in the photonic band structure. While for a single negative/positive constitutive parameters, there appear photonic band gaps, in the photonic band structure, originated from electric or magnetic resonance.

In the frequency range $0.05<\omega a/2\pi c<0.075$, both $\varepsilon_{\rm eff}$ and $\mu_{\rm eff}$ are positive, implying a positive refractive index, which corresponds to the first photonic band. Near to the frequency $\omega a/2\pi c=0.075$ resonances appear for both $\varepsilon_{\rm eff}$ and $\mu_{\rm eff}$, leading to the formation of the photonic band gap and the flat bands. Actually, the flat bands originate from spin-wave resonance, which corresponds to $\mu_{rs}=\mu'_{rs}=0$. From Eq. (2) it is easy to obtain the frequency of the spin-wave resonance $\omega_{\rm spin}=\sqrt{\omega_0(\omega_0+\omega_m)}=0.08\cdot 2\pi c/a$, which locates at the top of the flat bands in Fig. 2(a). After the spin-wave resonance $\varepsilon_{\rm eff}$ and $\mu_{\rm eff}$ become positive again, corresponding to the photonic band in frequency regime $0.08<\omega a/2\pi c<0.1$. At the frequency near to 0.1 another $\mu_{\rm eff}$ resonance appears, corresponding to the flat bands and the photonic band gap nearby in Fig. 2(a). The resonance arises from the magnetic surface-plasmon resonance of the ferrite rod, which was discussed detailedly in literature.[28] Above the resonance both $\mu_{\rm eff}$ and $\varepsilon_{\rm eff}$ are positive until the appearance of the second $\varepsilon_{\rm eff}$ resonance, which correspond to the photonic band in the frequency regime $0.12<\omega a/2\pi c<0.24$ and the photonic band gap above, respectively.

Approximate the ferrite material as an isotropic medium with permeability $(\mu_{rs}^2-\mu_{\kappa s}^2)/\mu_{rs}$, we also calculate the corresponding effective constitutive parameters and photonic band structure, as shown in Figs. 2(d) and 2(c), respectively. The effective constitutive parameters and the photonic band structure are in good agreement with each other as well. Different from the anisotropic case, the second $\mu_{\rm eff}$ resonance do not induce the photonic band gap because of the degeneracy at high-symmetry point M. Comparing Figs. 2(b) and 2(d), we can find except the frequency regime around the second $\mu_{\rm eff}$ resonance, the results are nearly the same, which can also be seen by comparing Figs. 2(a) and 2(c). It is indicated that in the usual case it is a reasonable approximation to take the permeability of the ferrite material as an isotropic one, while in the frequency regime around the surface-plasmon resonance to ensure the accuracy of the EMT, the anisotropy of the ferrite material must be considered.

The EMT is the method operating at long wavelength limit, consequently, we have calculated the photonic band structures near the Γ point with the MST and the EMT, as shown in Fig. 3(a) where the red solid lines are the results from the EMT and the blue circles correspond to those from the MST. The effective constitutive parameters calculated with the EMT are presented as well in Fig. 3(b) where the red solid line and the blue dashed line correspond to the effective permittivity and effective permeability, respectively. The parameters used are the same as those in Figs. 2(a) and 2(b). It can be seen from Fig. 3(a) that for the frequency $\omega a/2\pi c<0.1$ the photonic band structures from two methods are almost the same, suggesting the accuracy of the developed EMT. For the last band at the frequency $\omega a/2\pi c>0.16$ the difference appears near the zone boundary. However, it does not mean the EMT is not effective since it locates near to the electric resonance where $k_{\rm eff}r_0$ does not satisfy the condition $k_{\rm eff}r_0 \ll 1$. Actually, our results suggest that even when a/λ_0 approaches to 0.4 and $k_0 r_s=0.6$ the EMT is still effective.

IV. MERITS OF THE EMT FOR THE ANISOTROPIC MM

To investigate the effect of anisotropy on the optical properties of the anisotropic MM. At frequency $f=4$ GHz we have performed the simulations on the electric field intensity patterns of a plane wave illuminated on a cylinder composed of anisotropic MM with radius $R=10a$ and an equal-size effective cylinder with the effective permittivity $\varepsilon_{\rm eff}=4.1+i9\times10^{-4}$ and the effective permeability $\mu_{\rm eff}=-0.8+i7\times10^{-3}$ defined by Eq. (9) with $\mu_{re}=0.4+i1\times10^{-3}$ and $\mu_{\kappa e}=0.7+i9\times10^{-4}$. The ferrite rods involved possess the same parameters as in Fig. 2, in addition, the absorption is considered as well by taking the damping coefficient $\alpha=3\times10^{-4}$

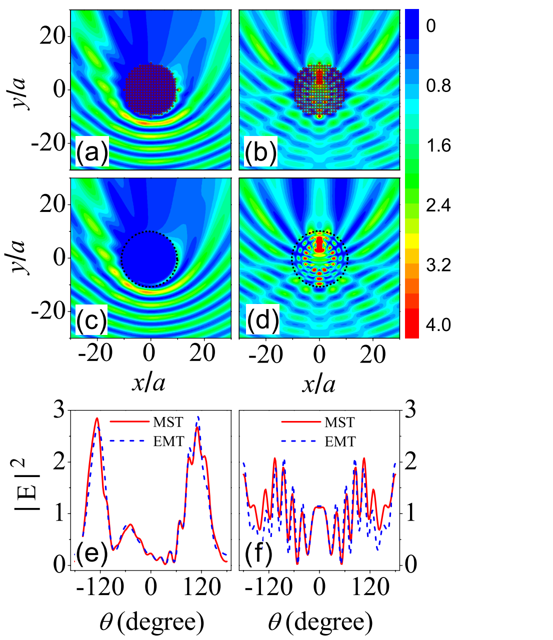

FIG. 4. (Color online) (a) The electric field intensity pattern of a plane wave illuminated on a cylinder composed of anisotropic MM with radius $R=10a$ and (c) its equal-size effective one. (b) The corresponding electric field intensity pattern of a plane wave illuminated on the cylinder composed of isotropic MM with radius $R=10a$ and (d) its equal-size effective one. The electric field intensity around the circles with the radius $R'=15a$ in panels (a), (c), and (b), (d) are presented in panels (e) and (f), respectively. The red solid lines and the blue dashed lines correspond to the electric field in panels (a) and (b), and panels (c) and (d), respectively.

and the permittivity $\epsilon_s=15+i3\times10^{-3}$. The results are shown in Figs. 4(a) and 4(c), respectively, where the ferrite rods that make up the anisotropic MM are denoted with the circles as shown in Fig. 4(a), while the boundary of the effective cylinder is marked with the dotted circle as shown in Fig. 4(c). Compared Figs. 4(a) and 4(c), it is obvious that the electric field intensity patterns are almost the same, indicating the effectiveness and the accuracy of the EMT. Moreover, the asymmetry of the pattern confirms the necessity to take account of the anisotropy of the permeability. To examine quantitatively the effect of the anisotropy of MM on the optical properties, the electric field intensity around the circles with radius $R'=15a$ for panels (a) and (c) are plotted in Fig. 4(e), where the red solid line and the blue dashed line are the results corresponding to panels (a) and (c), respectively. Note in passing that the angle θ is defined in the manner that positive y axis is taken as 0° for the convenience of comparison. It can be seen clearly that the results from EMT recover exactly those from the rigorous MST, which suggests once again the accuracy and the robustness of the developed EMT.

By approximating the ferrite rod as an isotropic material with the permeability $\mu_s=(\mu_{rs}^2-\mu_{\kappa s}^2)/\mu_{rs}$, we also present the electric field intensity patterns of the cylinder composed of isotropic MM with radius $R=10a$ and the equal-size effective cylinder with the effective permittivity $\varepsilon_{\text{eff}}=3.3+i\eta$ and the effective permeability $\mu_{\text{eff}}=2.2+i3\times10^{-3}$, as shown in Figs. 4(b) and 4(d), respectively, where η is a negligibly small quality $\sim10^{-5}$. The corresponding quantitative results around the circles with radius $R'=15a$ are given as well in Fig. 4(f). By comparing panels (b), (d), and the red solid, blue dashed lines in panel (f), it can be seen that the results are in good agreement with each other. However, the electric field intensity pattern corresponding to the realistic system [panel (a)] cannot be recovered, indicating that approximating ferrite as an isotropic material is incorrect at this frequency. Examining the effective constitutive parameters, we can find when considering the permeability as a tensor, the effective permittivity and permeability obtained from the EMT are positive and negative, respectively, suggesting the appearance of a photonic band gap as shown in Fig. 2(a) at $\omega a/2\pi c=0.107$. Accordingly, the electric field intensity inner the cylinder is nearly zero. Nonetheless, when considering the permeability as an isotropic one, the effective constitutive parameters are both positive, corresponding to the photonic band as shown in Fig. 2(c), suggesting a field pattern inner the cylinder. Consequently, it is necessary to take account of the gyromagnetic property of the ferrite rod instead of approximating it as an isotropic one.

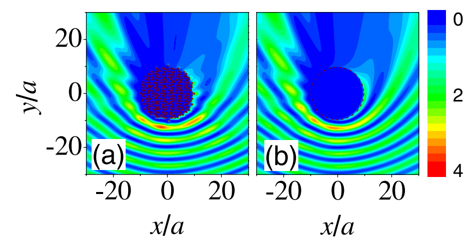

FIG. 5. (Color online) The electric field intensity patterns of a plane wave illuminated on a cylinder composed of anisotropic MM with radius $R=10a$ (a) and its equal-size effective one (b). Different from Fig. 4(a), position disorder of the ferrite rods has been introduced for the anisotropic MM. Actually, (b) is Fig. 4(c), presented here is just for the comparison with (a).

In the EMT, the anisotropic MM is considered as a homogenous anisotropic EM medium, accordingly, the effective constitutive parameters retrieved from the EMT do not depend on the lattice structure of the ferrite rods. For this reason we can expect that the EMT is still effective even when position disorder of the ferrite rods is introduced. To examine the issue we have performed the simulation on the electric field intensity pattern of a plane wave illuminated on a cylinder composed of anisotropic MM with radius $R=10a$. Position disorder is introduced in the manner that the displacement of each ferrite rod from its original position is defined as $d_i=\xi\cdot\eta\cdot d_{i0}$ with $i=x$ or y, ξ is the random numbers uniformly distributed between -0.5 and 0.5, η is the quantity measuring the degree of disorder, and $d_{i0}=a-2r$ is the maximum variation in the position within a unit cell for a square lattice. The result is given in Fig. 5(a) where the disordered circles denote the ferrite rods with the degree of the position disorder $\eta=1$ to avoid the overlap of the neighboring ferrite rods and the other parameters are the same as those in Fig. 4(a). The electric field intensity pattern of its equal-size effective one is also presented in Fig. 5(b) for comparison. It is obvious that except the local field near to the ferrite rods around the boundary, the electric field intensity patterns in Figs. 5(a) and 5(b) bear close resemblance, suggesting the effectiveness of the EMT for anisotropic MM with disorder involved. It is noted that the electric intensity pattern is also similar to that of the anisotropic MM without disorder as shown in the Fig. 4(a), which can be justified from the fact that the average filling ratios of the ferrite rods in the above two configurations are the same. In addition, the EM wave cannot discern the position variation in the ferrite rods in the long wave limit so that for a fixed rod the scattering from all the other rods can be considered as a homogenous background in the coherent-potential approximation.

V. CONCLUSION

In conclusion, we have developed an effective-medium theory for the anisotropic MM, which is proved to be powerful in retrieving the effective constitutive parameters. Comparison between the photonic band-structure calculations and the theory suggests that the EMT applies very well when $a/\lambda_0 < 0.3$ and $k_0 r_s = 0.6$, and even when a/λ_0 is close to 0.4 and the disorder is introduced the theory is still in good agreement with the photonic band-structure calculations. In addition, it is suggested that in the usual case it is a reasonable approximation by taking the ferrite as an isotropic material with permeability $(\mu_r^2 - \mu_\kappa^2)/\mu_r$, however, at the frequency around the magnetic surface-plasmon case is different. Consequently, to understand the optical properties of anisotropic MM correctly it is necessary to take the gyromagnetic property of the ferrite material exactly into account.

ACKNOWLEDGMENTS

This work was supported by the China-973 program, NNSFC, PCSIRT, MOE of China (Grant No. B06011), and Shanghai Science and Technology Commission. S.T.C. is partly supported by the U.S. DOE.

*Author to whom correspondence should be addressed; 072019008@fudan.edu.cn

[1] V. C. Veselago, Sov. Phys. Usp. **10**, 509 (1968).
[2] J. B. Pendry, Phys. Rev. Lett. **85**, 3966 (2000).
[3] D. R. Smith, W. J. Padilla, D. C. Vier, S. C. Nemat-Nasser, and S. Schultz, Phys. Rev. Lett. **84**, 4184 (2000); R. A. Shelby, D. R. Smith, S. C. Nemat-Nasser, and S. Schultz, Appl. Phys. Lett. **78**, 489 (2001); R. A. Shelby, D. R. Smith, and S. Schultz, Science **292**, 77 (2001).
[4] S. Zhang, W. Fan, N. C. Panoiu, K. J. Malloy, R. M. Osgood, and S. R. J. Brueck, Phys. Rev. Lett. **95**, 137404 (2005).
[5] G. Dolling, C. Enkrich, M. Wegener, C. M. Soukoulis, and S. Linden, Science **312**, 892 (2006).
[6] L. Peng, L. Ran, H. Chen, H. Zhang, J. A. Kong, and T. M. Grzegorczyk, Phys. Rev. Lett. **98**, 157403 (2007).
[7] F. J. Rachford, D. N. Armstead, V. G. Harris, and C. Vittoria, Phys. Rev. Lett. **99**, 057202 (2007).
[8] S. Liu, W. Chen, J. Du, Z. Lin, S. T. Chui, and C. T. Chan, Phys. Rev. Lett. **101**, 157407 (2008).
[9] S. Zhang, Y. S. Park, J. Li, X. Lu, W. Zhang, and X. Zhang, Phys. Rev. Lett. **102**, 023901 (2009).
[10] A. K. Sarychev, R. C. McPhedran, and V. M. Shalaev, Phys. Rev. B **62**, 8531 (2000).
[11] D. R. Smith, S. Schultz, P. Markoš, and C. M. Soukoulis, Phys. Rev. B **65**, 195104 (2002); T. Koschny, P. Markos, D. R. Smith, and C. M. Soukoulis, Phys. Rev. E **68**, 065602(R) (2003); D. R. Smith, D. C. Vier, T. Koschny, and C. M. Soukoulis, *ibid.* **71**, 036617 (2005); T. Koschny, P. Markoš, E. N. Economou, D. R. Smith, D. C. Vier, and C. M. Soukoulis, Phys. Rev. B **71**, 245105 (2005).
[12] X. Chen, T. M. Grzegorczyk, B. I. Wu, J. Pacheco, and J. A. Kong, Phys. Rev. E **70**, 016608 (2004).
[13] V. B. Bregar, Phys. Rev. B **71**, 174418 (2005).
[14] Y. Wu, J. Li, Z. Q. Zhang, and C. T. Chan, Phys. Rev. B **74**, 085111 (2006).
[15] Z. Li, K. Aydin, and E. Ozbay, Phys. Rev. E **79**, 026610 (2009).
[16] O. Ouchetto, C. W. Qiu, S. Zouhdi, L. W. Li, and A. Razek, IEEE Trans. Microwave Theory Tech. **54**, 3893 (2006).
[17] J. B. Pendry, A. J. Holden, W. J. Stewart, and I. Youngs, Phys. Rev. Lett. **76**, 4773 (1996).
[18] J. B. Pendry, A. J. Holden, D. J. Robbins, and W. J. Stewart, IEEE Trans. Microwave Theory Tech. **47**, 2075 (1999).
[19] Z. Wang, Y. D. Chong, J. D. Joannopoulos, and M. Soljačić, Phys. Rev. Lett. **100**, 013905 (2008).
[20] D. M. Pozar, *Microwave Engineering*, 3rd ed. (Wiley, New York, 2004).
[21] S. T. Chui and L. B. Hu, Phys. Rev. B **65**, 144407 (2002).
[22] P. Sheng, *Introduction to Wave Scattering, Localization, and Mesoscopic Phenomena* (Academic, San Diego, 1995).
[23] X. Hu, C. T. Chan, J. Zi, M. Li, and K. M. Ho, Phys. Rev. Lett. **96**, 223901 (2006).
[24] X. Hu, K. M. Ho, C. T. Chan, and J. Zi, Phys. Rev. B **77**, 172301 (2008).
[25] Y. Wu, Y. Lai, and Z. Q. Zhang, Phys. Rev. B **76**, 205313 (2007).
[26] J. Xu, R. X. Wu, P. Chen, and Y. Shi, J. Phys. D **40**, 960 (2007).
[27] C. F. Bohren and D. R. Huffman, *Absorption and Scattering of Light by Small Particles* (Wiley, New York, 1983).
[28] S. Liu, J. Du, Z. Lin, R. X. Wu, and S. T. Chui, Phys. Rev. B **78**, 155101 (2008).